

ATI 2015 - 70th Conference of the ATI Engineering Association

## A conjugate-heat-transfer immersed-boundary method for turbine cooling

D. De Marinis<sup>a</sup>, M. D. de Tullio<sup>a</sup>, M. Napolitano<sup>a,\*</sup> and G. Pascazio<sup>a</sup>

<sup>a</sup>*Department of Mechanical, Mathematic and Management, Polytechnic of Bari, via Re David 200, 70125, Bari, Italy.*

### Abstract

The first high pressure stage of a modern gas turbine operates at very high temperatures that require complex blade-cooling systems to guarantee high performance and efficiency of the gas turbine while maintaining a very low level of energy losses, though using compressed air for cooling.

An accurate and efficient conjugate heat transfer (CHT) solver is thus necessary to compute the flow and temperature fields of the air within the cooling channels and of the gas around the blades—by means of the Navier—Stokes and energy equations—as well as the blade temperature field, by means of the heat conduction equation. Due to the very high geometrical complexity of the cooling channels within the blades, generating a body fitted mesh for the three domains—air, gas and blade—is extremely difficult and time consuming. Nevertheless, many turbine blade-cooling simulations have been performed with success, though at large computational cost, see, e.g., [1].

A promising alternative approach is provided by the Immersed Boundary (IB) method, which discretizes both the solid and fluid fields by means of a single Cartesian grid, thus reducing the grid generation process to a relatively simple and quick task—an interesting review of the IB method and its application is provided in [2].

The CFD group at the Department of Mechanics, Mathematics and Management of the Polytechnic of Bari has chosen such an approach, by first developing and improving an accurate and efficient IB method for the compressible Navier—Stokes equations [3, 4], and later extending it with success to solve CHT problems [5]. At present, these works are limited to two-dimensional serial calculations.

The aim of this work is to extend the two-dimensional IB solver to three-dimensions, using a new IB least-squares reconstruction, an advanced data structure and a parallel solver, so as to obtain a computational tool capable of computing very complex CHT problems within reasonable computational times.

© 2015 The Authors. Published by Elsevier Ltd. This is an open access article under the CC BY-NC-ND license (<http://creativecommons.org/licenses/by-nc-nd/4.0/>).

Peer-review under responsibility of the Scientific Committee of ATI 2015

*Keywords:* URANS , Immersed Boundary Method, Conjugate Heat Transfer, Turbine Cooling

\* Corresponding author: Tel.: + 390805963464; fax: + 390805963464,  
*E-mail address:* [michele.napolitano@poliba.it](mailto:michele.napolitano@poliba.it)

## 1. Numerical solver

The compressible Unsteady Favre-Averaged Navier–Stokes (URANS) equations, combined with the  $\kappa$ - $\omega$  turbulence model proposed by Wilcox [6], are written in vector form and discretized in time using three point backward differences, the molecular viscosity being computed by Sutherland’s law. A pseudo-time derivative premultiplied by the preconditioning matrix proposed by Merkle [7] is added to the left-hand-side of the vector equation in order to use a time marching approach, which is robust and efficient for a wide range of the Mach number, for both steady and unsteady problems. The pseudo-time derivative is discretized using a backward Euler scheme and the resulting time discretized equation is written in delta form. In order to solve the resulting linear system, the diagonalization procedure of Pulliam & Chaussee [8] is used. In this way the BiCGStab solver, instead of being applied to a huge matrix, is applied three times to much smaller matrices each containing the diagonal terms and the off-diagonal ones associated to one space direction. As far as the spatial discretization is concerned, a collocated, cell-centred finite volume space discretization is used. A second-order-accurate upwind differencing scheme is used to discretize the convective terms in the right-hand-side residual; the viscous terms are approximated by second-order-accurate central differences; and the convective term in the left-hand-side is always discretized using a first-order upwind scheme (deferred-correction approach) in order to increase the diagonal dominance of the linear systems to be solved. A minmod limiter is used around shocks. Finally, the boundary conditions are treated explicitly.

A complete description of the solver is given in [4].

## 2. Immersed Boundary method based on a least squares reconstruction scheme

The IB method allows one to greatly simplify the grid generation and even to automate it completely. The governing equations are solved directly on a Cartesian grid in their simplest form by means of very efficient numerical schemes that can be also parallelized in a relatively simple way. On the other hand, the effect of the body has to be accounted for and the relative position of each grid cell with respect to the body has to be determined. This is accomplished by a ray-tracing algorithm; the grid generator detects the cell faces that are cut by the body surface and divides the cells into three types: solid and fluid cells, whose centres lie within the body and within the fluid, respectively; and fluid/solid interface cells, which have at least one of their neighbours inside the body/fluid. Furthermore, the ray-tracing procedure allows one to generate a locally refined grid very easily, so as to use a fine grid in the high-flow-gradient regions and a coarser one where the flow is smooth. Then, the centres of the fluid- and solid-interface cells are projected onto the body surface along its normal direction, so as to obtain fluid-cells projection points (FCPP) and solid-cell projection points (SCPP), (see Fig. (1a)).



Fig. 1: Immersed Boundary: ray-tracing technique and generation of FCPPs and SCPPs (a); reconstruction scheme (b).

The boundary conditions, which account for the presence of the body, are mimicked by a special treatment of the interface cells, according to the direct forcing procedure [9]. A local interpolation procedure is used to transfer the boundary conditions onto the centers of the fluid/solid interface cells, whereas the governing equations are solved at all of the fluid/solid cell centers and the solid/fluid cells have no influence whatsoever on the fluid/solid domain.

The interpolation procedure proposed here needs, for each interface cell, the imposed values of the variables at the wall and the values of the variables at a probe placed along the local wall normal and distant  $\delta$  from the wall.

The choice of distance  $\delta$  is obviously critical for the application of this procedure and in the present work  $\delta$  has been fixed equal to twice the largest distance between the interface cells and the wall.

An interpolation procedure using  $ne$  contiguous cells is needed to compute the variables at the probe, since the wall normal passing through the interface cell could not intersect any computational node. Following the idea of Vanella and Balaras [10], a support-domain around each probe is defined and a shape function, based on a moving least-squares approach, is constructed in it.

Finally a zero pressure gradient in the wall normal direction is imposed and the velocity, the temperature and the turbulence variables are linearly interpolated using the values at the wall and at the probe, see Fig. (1b).

### 3. Conjugate Heat Transfer

In CHT problems, the URANS equations are solved at all internal fluid cells, whereas the heat conduction equation is solved at all internal solid cells using the same spatial discretization and time-marching numerical algorithm; the interface boundary conditions require that both the temperature and heat-flux are the same for the fluid and the solid at all boundary points:

$$T_{w,f} = T_{w,s} \quad \kappa_s \nabla T_s \cdot \mathbf{n}_w = \kappa_f \nabla T_f \cdot \mathbf{n}_w \quad (1 \text{ a, b})$$

where the subscripts  $s$  and  $f$  refer to solid and fluid respectively,  $\kappa$  indicates the thermal conductivity, and  $\mathbf{n}_w$  is the unit vector normal to the wall. In order to impose the boundary conditions above, at the solid interface cells the effect of the boundary conditions imposed by the flow upon the temperature and heat-flux at the body surface has to be accounted for, exactly as the same conditions are to be enforced at the fluid-interface cells. Since the FCPPs and the SCPPs in general do not coincide (see Fig. (1a)), a connectivity map for all FCPPs and SCPPs on the surface is to be created.

A direct coupled solution of the URANS and heat conduction equations is unfeasible. Thus, an iterative procedure is to be employed. A first-order-accurate approximation of  $\nabla T_f \cdot \mathbf{n}_{w,f}$  is obtained as:

$$\nabla T_f \cdot \mathbf{n}_{w,f} = (T_{int,f}^m - T_{w,f}^{m-1}) \beta_f \quad (2)$$

where  $m$  is the current iteration and  $\beta_f$  is the inverse of the distance between the fluid interface cell and the wall. Eq. (2) provides the heat fluxes (apart from the thermal conductivity) at all FCPPs. Such values are then used to provide those pertaining to all SCPPs by means of a distance-weighted interpolation and then, the Neumann condition at all SCPPs is written as:

$$\nabla T_s \cdot \mathbf{n}_{w,s} = \frac{\kappa_f}{\kappa_s} (\nabla T_f \cdot \mathbf{n}_{w,f}) = \frac{\kappa_f}{\kappa_s} \sum_i^{ns} \frac{a_i}{q} (\nabla T_f \cdot \mathbf{n}_{w,f})|_i, \quad (3)$$

where  $ns$  is the number of the neighboring FCPPs,  $a_i$  is the inverse of the distance between the considered SCPP and the surrounding FCPP $_i$  and  $q = \sum_i^{ns} a_i$ .  $T_{w,s}^m$  can then be computed using again a first-order-accurate scheme:

$$T_{w,s}^m = T_{int,s}^m - \frac{\nabla T_s \cdot \mathbf{n}_{w,s}}{\beta_s}, \quad (4)$$

and used to provide the wall fluid temperature at all SCPPs by means of the Dirichlet condition. Such values are finally interpolated onto the FCPPs to provide the updated value for  $T_{w,f}^m$ :

$$T_{w,f}^m = \sum_i^{nf} \frac{a_i}{q} (T_{w,f}^m)|_i = \sum_i^{nf} \frac{a_i}{q} (T_{w,s}^m)|_i, \quad (5)$$

where  $nf$  is the number of the neighboring SCPPs,  $\alpha_i$  is the inverse distance between the considered FCPP and the surrounding SCPP $_i$  and  $q = \sum_i^{nf} \alpha_i$ .

## 4. Results

### 4.1. Conjugate heat transfer in a rotating flow inside a tube

The heat transfer problem in a rotating flow inside a tube has been considered at first to validate the present approach. The fluid is contained between a stationary hollow inner cylinder and a rotating outer one. The outer cylinder has a radius  $R_o = 1.8$  m, moves with tangential velocity  $U_o = 5$  m/s and is kept at  $T_o = 700$  K. The inner hollow cylinder has radii equal to  $R_m = 0.9$  m and  $R_i = 0.45$  m, respectively, the inner surface is kept at  $T_i = 500$  K and  $\kappa_s/\kappa_f = 9$ . An analytical solution is available for the two-dimensional Navier—Stokes equations with the above conditions and it is reported in [5].

Computations have been performed using  $ns$  and  $nf$  both equal to 7, periodic boundary conditions in the axial direction—to solve a 2D flow by a 3D code—and a uniform Cartesian grid with  $\Delta x = \Delta y = 0.04, 0.02, 0.01, 0.005$ . The solution well provides the (tangential component of the) velocity and temperature fields within the flow and the hollow tube. Fig. (2) shows the four grid results for the wall temperature at  $R_m$  (a) and the velocity (b) and temperature (c) radial distributions obtained with the finest grid  $\Delta x = \Delta y = 0.005$ . The exact analytical solutions are also reported for comparison. The numerical solution tends to the analytical one when refining the mesh and the finest grid one has a maximum error less than 0.2 %.

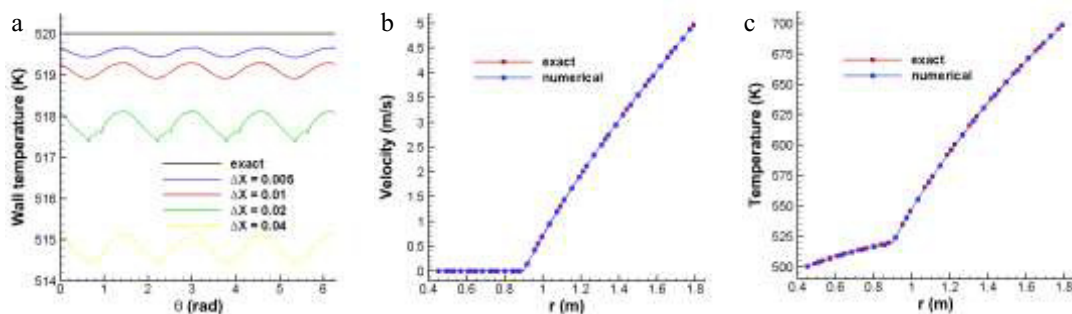


Fig. 2: Rotating flow: wall temperature distribution (a); radial velocity distribution (b); radial temperature distribution (c).

#### 4.2. Conjugate heat transfer in an internally cooled C3X vane.

The flow past the C3X turbine guide vane of Hylton et al. [11] was selected as a very severe test case, for which detailed experimental results are also available.

The three-dimensional computational domain included one vane, with periodic boundary conditions employed to simulate the cascade test condition, as well as 10 cooling channels. The domain extended from the hub to the shroud, the computational inlet was located at about one chord length upstream of the vane leading edge, while the computational exit at about one chord length downstream of the vane trailing edge.

The operating conditions, listed in Tab. (1), are the ones of the test-case R112 documented in [11]. The hot gas total pressure  $P_{t,in}^h$  and total temperature  $T_{t,in}^h$  were specified at the inlet where the turbulence intensity was imposed to be the experimental value of 8.3%. The static pressure  $P_{s,out}^h$  (derived using  $P_{t,in}^h$  and  $Ma_{out}^h$ ) was specified at the exit. The coolant flows in the ten channels are independent of each other and fully developed at the channel inlet (i.e., the hub of the vane), being fed by long tubes. The mass flow rates FR (reported in [11]) and hub total temperatures  $T_{t,in}^c$  and pressures  $P_{t,in}^c$  for each channel are listed in Tab. (2),  $P_{t,in}^c$  and  $T_{t,in}^c$  being specified to match the corresponding flow rate. A static pressure  $P_{s,out}^c$  equal to 1 bar was imposed at the exit of the channels. Finally, the vane material is stainless steel (ASTM Type 310), with thermal conductivity  $\kappa = 0.0182 T + 6.13$ .

Table 1. Flow conditions of the R112 test-case.

$P_{t,in}^h$ (bar)	$T_{t,in}^h$ (K)	$Ma_{out}^h$	$P_{s,out}^h$ (bar)	$Tu_{in}$ (%)
3.217	783.0	0.90	1.925	8.3

Table 2. Coolant flow conditions of the R112 test-case.

Coolant (#)	Diameter (mm)	$P_{t,in}^c$ (bar)	$T_{t,in}^c$ (K)	$P_{s,out}^c$ (bar)	FR (g/s)
1	6.30	1.539	412.2	1.0	7.79
2	6.30	1.386	408.7	1.0	6.58
3	6.30	1.336	389.0	1.0	6.34
4	6.30	1.386	396.0	1.0	6.66
5	6.30	1.351	372.1	1.0	6.50
6	6.30	1.420	435.4	1.0	6.72
7	6.30	1.344	384.2	1.0	6.33
8	3.10	2.015	372.3	1.0	2.26
9	3.10	1.449	420.0	1.0	1.38
10	1.98	1.872	433.2	1.0	0.68

Results have been obtained with three meshes having a total number of cells equal to 368104, 1472416 and 2208624 cells. The base Cartesian grids have:  $\Delta z = 0.025$  m always;  $\Delta x$  and  $\Delta y = 0.015$  m, 0.0075 m and 0.005 m, respectively. The grids are smaller within the holes and the vanes and are locally refined, as shown in Fig. (3a), where the finest grid at mid-span is shown. It is noteworthy that the periodic boundary conditions simulating the cascade test condition can be imposed within the IB method even if the vane height is larger than the vane spacing. Fig. (3b) and (3c) provide the computed and measured mid-span pressure and temperature distributions on both sides of the vane, respectively; Fig. (3d) finally shows the temperature contours for three different z-planes. The computed pressure distribution is grid converged and satisfactory. The computed wall temperature tends towards the experimental one when refining the mesh, but is not yet grid-converged. The largest discrepancies are encountered near the leading edge where an adequate resolution is crucial to correctly capture the thermal field. For this reason, current

work aims at implementing velocity and temperature wall functions, which are expected to provide more accurate results for a given grid.

## 5. Conclusions and future work

An accurate and efficient two-dimensional CHT-IB method, employing a local grid refinement and an IB distance-weighted reconstruction, has been extended to three dimensions and equipped with: a new IB least-squares reconstruction; an advanced data structure; and a parallel solver. The code has been tested versus: i) rotating flow inside a tube; ii) flow past a cascade of internally cooled C3X turbine vanes. Current work aims at implementing velocity and temperature wall functions, which are expected to provide more accurate results for a given grid.

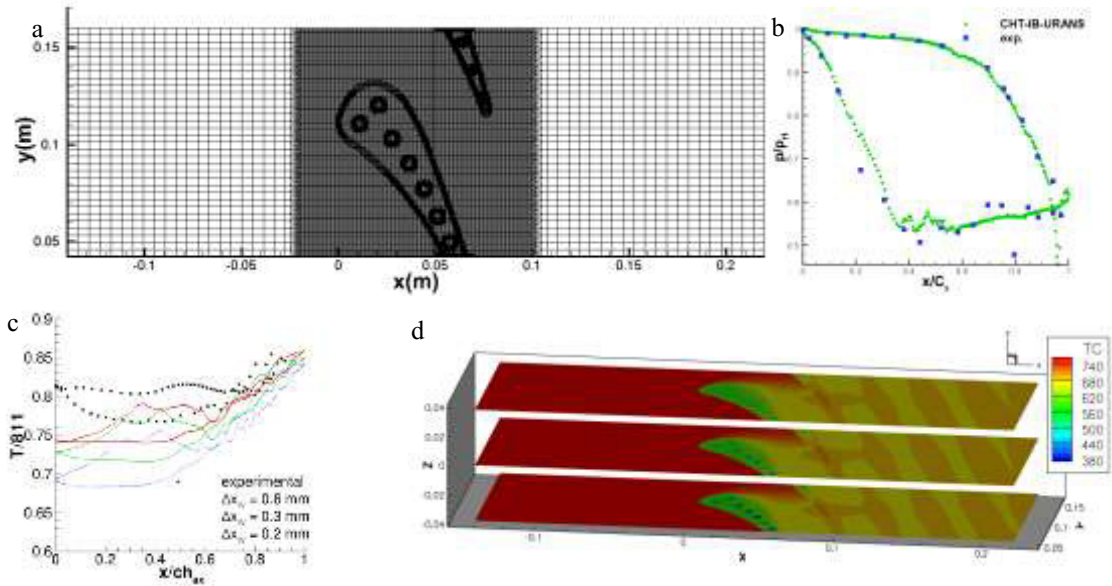


Fig. 3: C3X vane: locally refined grid (a); mid-span pressure (b) and temperature (c) distribution on the external surface of the vane; temperature contours for three different z-planes (d).

## References

- [1] Luo G. and Razinsky E. H., *Conjugate heat transfer analysis of a cooled turbine vane using the V2F turbulence model. Journal of Turbomachinery*, 129(4):773 (2007);
- [2] Mittal R. and Iaccarino G., *Immersed boundary methods. Annual Review of Fluid Mechanics*, 37, 239 (2005);
- [3] De Palma P., de Tullio M. D., Pascazio G. and Napolitano M., *An immersed-boundary method for compressible viscous flows. Computers & fluids*, 35:693 (2006);
- [4] de Tullio M. D., De Palma P., Iaccarino G., Pascazio G. and Napolitano M., *An immersed boundary method for compressible flows using local grid refinement. Journal of Computational Physics*, 225:2098 (2007);
- [5] de Tullio M. D., Latorre S. S., De Palma P., Napolitano M. and Pascazio G., *An immersed boundary method for solving conjugate heat transfer problems in turbomachinery. V European Conference on Computational Fluid Dynamics ECCOMAS CFD*, (2010);
- [6] Wilcox D. C., *Turbulence modeling for CFD. second ed.* DCW Industries; 2nd edition, (1998);

- [7] Merkle C. L., *Preconditioning methods for viscous flow calculations. Computational fluid dynamics review*, 1995:419–436, (1995);
- [8] Pulliam T. H. and Chaussee D. S., *A diagonal form of an implicit approximate-factorization algorithm. Journal of Computational Physics*, 39(2):347–363, (1981);
- [9] Mohd-Yusof J., *Combined immersed-boundary/B-spline methods for simulations of flow in complex geometries. Center for Turbulence Research, Annual Research Briefs*, 1997:317–327, (1997);
- [10] Vanella M. and Balaras E., *A moving-least-squares reconstruction for embedded-boundary formulations. Journal of Computational Physics*, 228(18):6617–6628, (2009);
- [11] Hylton L., Mihelc M., Turner E., Nealy D. and York R., *Analytical and experimental evaluation of the heat transfer distribution over the surfaces of turbine vanes. National Aeronautics and Space Administration NASA Lewis Research Center*, (1983).
-